Available online at www.sciencedirect.com
SCIENCE DIRECT®
Journal of Power Sources 144 (2005) 135–140
JOURNAL OF POWER SOURCES
www.elsevier.com/locate/jpowsour

Short communication

Carbonaceous deposits in direct utilization hydrocarbon SOFC anode

Hongpeng He*, John M. Vohs, Raymond J. Gorte

Department of Chemical Engineering, University of Pennsylvania, Philadelphia, PA 19104, USA

Received 15 November 2004; accepted 8 December 2004
Available online 15 February 2005

Abstract

Carbonaceous deposits formed in Cu-based SOFC anode compartment by exposing porous YSZ anodes to *n*-butane at elevated temperatures were studied using a combination of *V–I* curves, impedance spectroscopy, SEM, and TPO measurements. While short-term exposure of a porous YSZ matrix to *n*-butane at 973 K resulted in the deposition of electronically conducting carbonaceous film and therefore to enhance the fuel cell performance, the power density decays quickly in *n*-butane at temperature 1073 K or higher for long-term operation. SEM results indicate that the carbonaceous deposits arising from gas phase reaction have different morphology, and a dense layer composed of poly-aromatic rings has been formed on the porous anode surface. The dense layer could block the penetration of fuels to the anode and ions transfer to the three-phase boundaries where electrochemical reactions occur, resulting in the drop of the power density. TPO measurements revealed that the amount of carbonaceous deposits increased and the type of deposits changed with exposure time to *n*-butane. The stability of deposits increased with extending the exposure time according to the increased oxidation temperature. Steam can remove the carbonaceous deposits from the porous YSZ anode, but the reaction temperature was severely elevated compared to that of oxygen. The carbonaceous deposits can also be removed at 973 K by steam but the deposition of carbon will be controlled by the speed of removal and formation from the gas phase reaction.

Keywords: Cu-based anode; SOFC; Carbonaceous deposits; SEM; TPO

1. Introduction

It is well known that Ni-cermet composite is the most commonly used materials for solid oxide fuel cell (SOFC) anodes [1,2]. Ni provides high electronic conductivity, reasonably good high temperature stability, and high catalytic activity for steam reforming. Unfortunately, direct utilization of hydrocarbons is usually not possible in the absence of added steam due to the fact that Ni tends to catalyze the formation of carbon fibers. The problem of carbon fiber formation is particularly severe for hydrocarbons larger than methane. H_2O:C ratios, higher even than that predicted from thermodynamic considerations, must be maintained [3–5] in order to avoid plugging the reactor with carbon while operating with higher hydrocarbon fuels.

Carbon formation could be avoided by replacing Ni with electronic conductors that do not catalyze carbon formation, such as Cu [6–8] or conducting oxides [9–11]. It is difficult to achieve sufficient conductivity with oxides under the reducing conditions of the anode [12,13]. Our research has focused primarily on the development of anodes made from composites of Cu, ceria, and YSZ for direct utilization hydrocarbon fuels, without first reforming the fuel to syngas in that Cu does not catalyze the formation of carbon fibers in the presence of dry hydrocarbons in the way that Ni does. Due to the fact that Cu has a low catalytic activity for hydrocarbon oxidation, it is necessary to add ceria to the anode formulation in order to achieve reasonable power densities [14]. Because CuO and Cu_2O melt at the temperatures required for processing YSZ, the fabrication of Cu-based anodes has required the development of synthetic methods that are different from those used to produce Ni-cermet composites [6,7,14,15]. Rather than calcining mixtures of CuO_x and YSZ, the Cu cermets

* Corresponding author. Tel.: +1 215 898 7230; fax: +1 215 573 2093.
E-mail address: hongpeng@seas.upenn.edu (H. He).

0378-7753/$ – see front matter © 2005 Elsevier B.V. All rights reserved.
doi:10.1016/j.jpowsour.2004.12.029

are fabricated by first producing a highly porous YSZ matrix, adding Cu to the matrix with impregnation of Cu salts and then by low temperature calcination.

Recent research indicates that exposure of Cu–ceria–YSZ anodes to *n*-butane at 973 K can lead to a large increase in power density due to the formation of carbonaceous residues within the anode [15,16]. As discussed elsewhere [15], for cells with Cu contents of 20 wt.% or less, large increases were observed in the power densities for operation in H_2 after the anode had been exposed to *n*-butane. The enhancement decreases with increasing Cu content, implying that the deposits improve the connectivity of the metallic phase in the anode. Analysis of the compounds formed by passing *n*-butane over a Cu-plated surface at 973 K showed the formation of poly-aromatic compounds (e.g. anthracene and similar compounds) that were soluble in toluene but conjugated enough to provide electronic conductivity [17]. Temperature-programmed oxidation (TPO) measurements indicated that relatively small quantities, a few weight percent, were sufficient to affect performance and that these compounds could be oxidized and removed from the anode at much lower temperatures than would be possible for graphitic particles [18]. However, rather than enhance the power density, it was also found that the carbonaceous deposits formed at 1073 K or higher can deteriorate the performance for long-term operation.

In the present study, we further investigated the effect of carbonaceous deposits on anode performance. The results suggest that the deposits formed at 973 K for short time can enhance electronic conductivity, but the carbon layer deposited on the surface of anode could block the fuel feeding and oxygen ions transfer, resulting in a decline of the power density. The deposits can be removed by either air or steam, but the reaction temperature will be much elevated for the latter case.

2. Experimental

The methods used for preparing and testing fuel cells with Cu-based cermet anodes have been discussed in other papers [6,7,14,15] and described briefly here. YSZ powder (Tosoh, 8 mol% Y_2O_3) was mixed with distilled water, a dispersant (Duramax 3005, Rohm & Haas), binders (HA12 and B1000, Rohm & Haas), and pore formers (graphite and poly-methyl methacrylate (PMMA)). For the fuel cell measurements, this slurry was cast onto a green tape that had no pore formers and then calcined at 1823 K to give a bilayer YSZ wafer with a 600 μm porous layer and a 60 μm dense layer. SEM micrographs of the structure obtained using these pore formers have been reported elsewhere [19]. The next step in preparing the fuel cells involved attaching the cathode to the dense side of the YSZ bilayer described above. After the addition of 10 wt.% graphite to a 50:50 YSZ and LSM ($La_{0.8}Sr_{0.2}MnO_3$, Praxair Technologies) mixture, a glycerol slurry of the mixture was painted onto the bilayer and calcined to 1523 K to form the cathode. To prepare the anode, the porous YSZ layer was impregnated with a mixed, ethanol aqueous solution of $(NH_4)_2Ce(NO_3)_6$ (Alfa Aesar, ACS 99+%) and then calcined at 723 K to form CeO_2. After the impregnation with ceria, the porous layer was impregnated by aqueous solutions of $Cu(NO_3)_2{\cdot}3H_2O$ and then calcined at 723 K to decompose the nitrate. The final composition of the anode used in this study was 10 wt.% ceria and 20 wt.% Cu.

For fuel cell performance testing, Ag mesh was attached to the cathode with Ag paste and Au wire was attached to the anode with Au paste. Each cell, having a cathode area of 0.33 cm^2, was then sealed onto 1.0 cm alumina tubes using Au paste and a ceramic adhesive (Aremco, Ceramabond 552). Finally, the entire cell was placed inside a horizontal furnace and heated to 973 K at 2 K min^{-1}, with pure H_2 being fed to the anode at a flow rate of 40 mL min^{-1}. The performance of the cells was characterized by potential–current (*V*–*I*) curves and impedance spectrum. The spectra were measured in galvanostatic mode, using a dc current density of 330 mA cm^{-2} and an ac perturbation of 3 mA cm^{-2}.

Carbon deposits, typical of those expected to form in the fuel cell anode, were analyzed by TPO. First, we prepared a porous YSZ using the same procedures as that of anode matrix for fuel cell, but the slurry was cast into rectangular pieces to form 2 mm × 2 mm × 5 mm slab instead of tapes. After impregnation of 20 wt.% CeO_2 (no Cu), the samples were heated in flowing H_2 at 973 K, then exposed to flowing *n*-butane for various times at the same temperature. The samples were then placed in a separate flow reactor and heated at 10 K min^{-1} to 1173 K in a 20% O_2 stream in He carrier. The reactor effluent was analyzed using a mass spectrometer. The amount of carbon present in the sample was calculated from the weight change before and after exposure to *n*-butane. Except for oxygen, steam was also used to examine the reaction between H_2O and deposits. The stability of these carbonaceous compounds can be recognized by measuring the carbon removal with O_2/He or H_2O/He stream as a function of time and temperature.

Scanning electron microscopy (SEM, JEOL JSM-6400) was used to determine the overall morphology of the deposited carbonaceous film on the anode surface.

3. Results and discussion

3.1. Fuel cell performance

In a previous study, we have shown that exposure of Cu–ceria–YSZ anodes to *n*-butane at 973 K can lead to a large increase in performance due to the formation of carbonaceous residues within the anode [15,18]. Based on the fact that the enhancement is large for anodes with low Cu contents and small for anodes with high Cu contents, it was concluded that the carbonaceous residues enhance electronic conductivity within the anodes. Indeed, only ceria and carbonaceous deposits in the anode also shows reasonable performance,

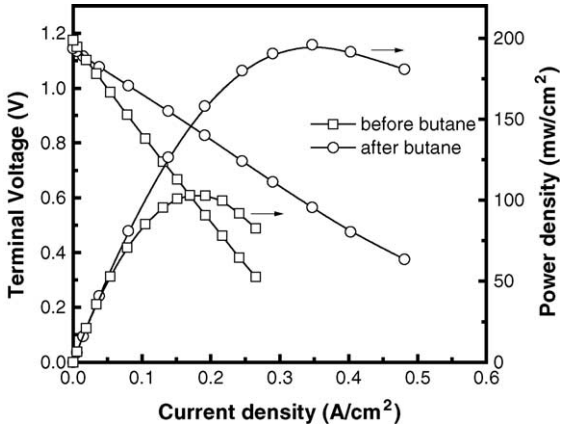

Fig. 1. Voltage and power density vs. current density curves utilizing H_2 fuel at 973 K for an anode containing 10 wt.% CeO_2 and 20 wt.% Cu before and after following 30 min exposure to *n*-butane.

which is very close to the value with 10 wt.% ceria and 20 wt.% Cu in anode. (Before exposure to *n*-butane, the fuel cell with only ceria in anode has negligible power density of several mW cm^{-2} because of no electronic conductor.) The effect of carbon deposits on fuel cell performance was shown in Fig. 1 with anode has 10 wt.% ceria and 20 wt.% Cu. The data were obtained in H_2 at 973 K before and after exposing the anode to *n*-butane for 30 min. Since 20 wt.% Cu is well below the Cu percolation threshold (∼30 wt.% Cu), the performance of typical cells with only 20 wt.% Cu is initially low due to poor connectivity within the metallic phase. The maximum power density of this cell doubles from 0.1 to almost 0.2 W cm^{-2} after exposure to *n*-butane because of improved electronic conductivity from carbon deposits that compensate the connection within the metallic phase.

Impedance spectra can verify the changes of microstructure in the anode before and after exposing to *n*-butane, so the corresponding impedance spectra were then recorded, which were shown in Fig. 2. As can be seen, the impedance spectra are composed of the electrolyte and electrode responses. The ohmic resistance decreased 0.82 Ω cm^2 from 1.41 to 0.59 Ω cm^2 after exposing to *n*-butane, which is very close to the resistance of YSZ at 973 K. The electrode responses are composed of two semicircles corresponding to high and low frequency semicircles, respectively. In the present study, the authors assume that the high frequency semicircle is not related to any chemical or electrochemical step but probably to the microstructure of electrodes and electrolyte–electrode interface. On the contrary, the low frequency semicircle is associated with the electrochemical reaction that occurs on the three-phase boundary. Since the cathode and electrolyte were identical in both cases, changes in the impedance spectra can be attributed only to changes in the anode. Clearly, the anode microstructure was greatly modified after exposing to *n*-butane, and the resistance decreased dramatically from 1.0 to 0.2 Ω cm^2. In the meanwhile, the electrochemical process was also enhanced, and the corresponding resistance decreased from 1.3 to 0.8 Ω cm^2.

It can be seen from the above analysis that the carbonaceous deposits can compensate the poor electronic conductivity of Cu because of sintering even for a short time exposure to *n*-butane. To further investigate the effect of carbonaceous residues, a cell with 10 wt.% ceria and 20 wt.% Cu in anode was operated for long-term in *n*-butane at 973, 1073 and 1173 K, respectively. The cell was initially heated to 973 K at 2 K min^{-1}, with pure H_2 being fed to the anode at a flow rate of 40 mL min^{-1}. Keep the cell at 973 K for 24 h in H_2 to stabilize the anode and then switch the fuel to *n*-butane. Current density was monitored as a function of time at different temperature while holding the cell potential at ∼0.5 V. As shown in Fig. 3, the cell performance is relatively stable at 973 K within the time of measurement (∼15 h), but declines quickly when operated at 1073 K and even more quickly at 1173 K, and eventually the fuel cell is almost shut down. The reasons of quick drop at 1073 K or above in *n*-butane may arise from several aspects. Firstly, since the carbonaceous deposits can enhance electronic conductivity within the anodes, so Cu sintering at 1073 K or above would not cause any problems. In fact, only ceria and carbonaceous deposits in the anode also shows the same drop in *n*-butane at 1073 K or above. Secondly, while ceria may deactivate at higher temperature, recent study reveals

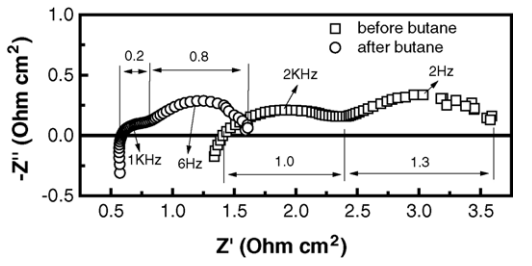

Fig. 2. Impedance spectra measured at 330 mA/cm^2 for an anode containing 10 wt.% CeO_2 and 20 wt.% Cu utilizing H_2 fuel at 973 K before and after following 30 min exposure to *n*-butane.

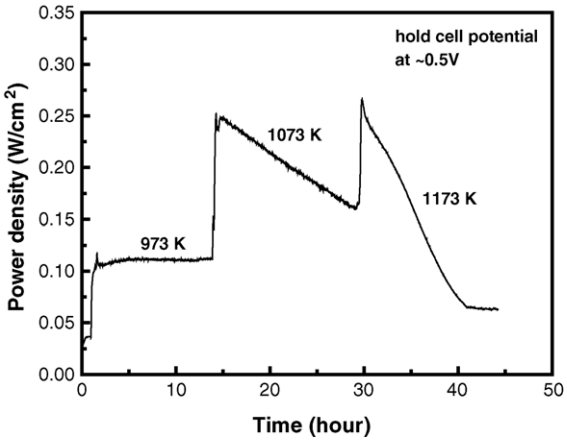

Fig. 3. Power density of a cell with anode containing 10 wt.% CeO_2 and 20 wt.% Cu utilizing butane at different temperature (hold cell potential at ∼0.5 V).

that the cell with anode contains 15 wt.% ceria and 35 wt.% Cu (in excess of the percolation limitation) shows very stable performance in H_2 at 1073 K. The result indicates that some loss of ceria catalytic activity would not cause the continuous drop of the performance in *n*-butane at 1073 K, so the carbonaceous residues formed by gas phase reaction would be the only reason for the quick drop of power density. Therefore, the nature of carbonaceous residues was further investigated.

3.2. Characterization of the carbonaceous deposits

After cell testing at 1173 K in *n*-butane, SEM images were recorded on the surface of anode to study the morphology of the carbonaceous deposits. Since Cu and ceria did not catalyze carbon formation, the deposits were formed totally from gas phase, free radical reaction. As shown in Fig. 4a, the carbon deposits have two kinds of morphology formed on the surface of anode. The small carbon balls agglomerated on the top are "flower-like" and stay loosely as in Fig. 4b, but the bottom layer along the anode surface seems dense as in Fig. 4c. The bottom layer in Fig. 4c was found to be composed of six-angle poly-aromatic rings as shown in Fig. 4d at higher magnification. It looks like that the small balls can transfer to poly-aromatic compounds continuously within the period of testing, therefore can broaden and densify the bottom layer. Clearly, the electronic conductivity can be greatly enhanced if the small carbon particles as in Fig. 4b dispersed within the anode, and therefore enhance the power density, but the dense layer at the bottom as shown in Fig. 4c and d may cause problems to the cell performance since the dense layer can only transfer electrons but block ions transfer and fuels feeding. The assumption can be verified by the fuel cell performance measurement, where the power density was found to be stable in *n*-butane for short-term but a continuous decline appeared for long-term, when the dense bottom layer formed.

The rate of deposits formation was measured by weight change before and after exposing to *n*-butane at 973 K with a small porous YSZ slab containing 20 wt.% ceria. Not surprisingly, the amount of the carbonaceous compounds increased with exposure time. As demonstrated in Fig. 5, there is a continuous increase in the amount of material deposited over the period of exposure. The amount increases from 0.5 wt.%

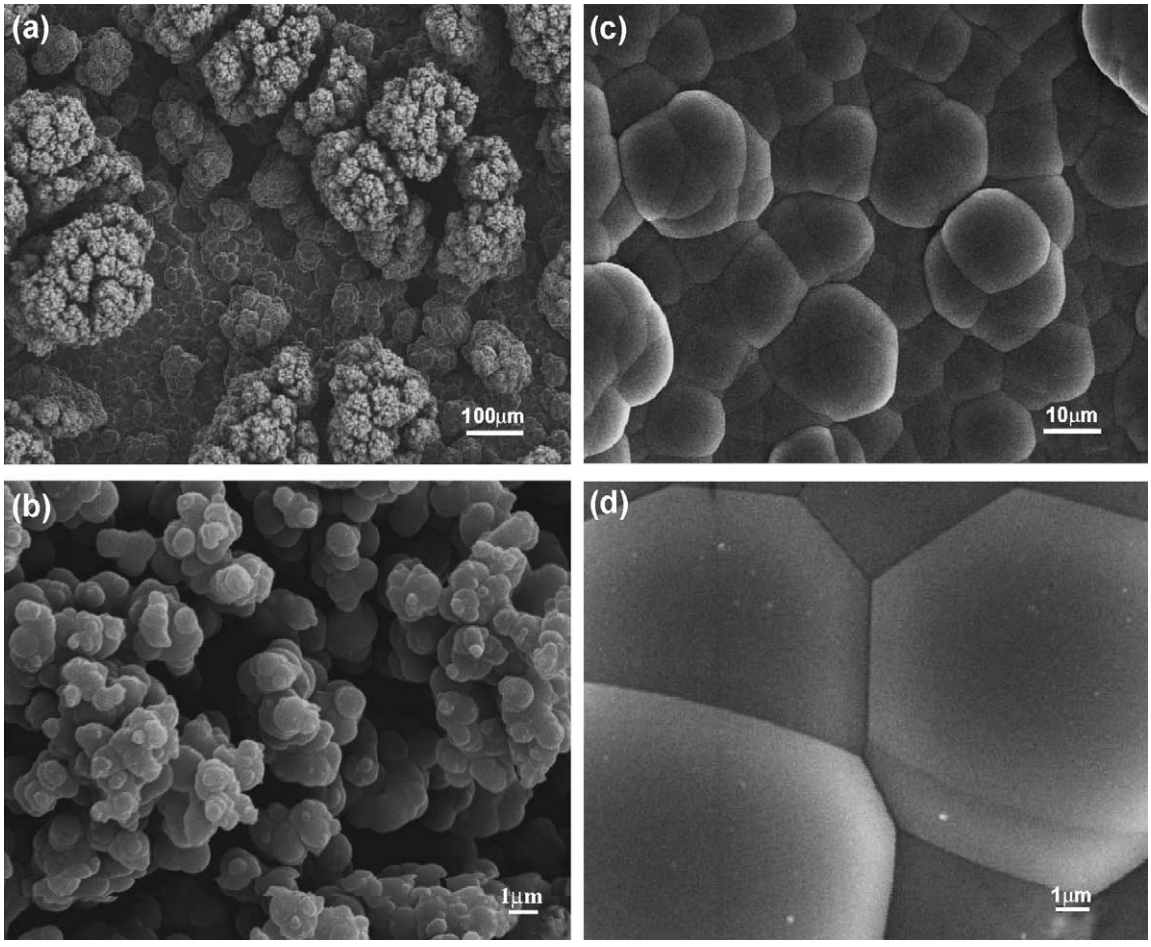

Fig. 4. The morphology of carbonaceous deposits on the surface of an anode containing 10 wt.% CeO_2 and 20 wt.% Cu after long-term testing in *n*-butane at 1173 K.

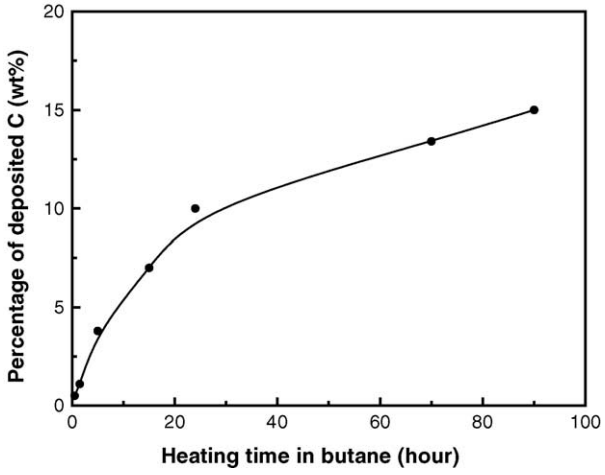

Fig. 5. The amount of carbonaceous deposits at 973 K after exposing to *n*-butane for different times.

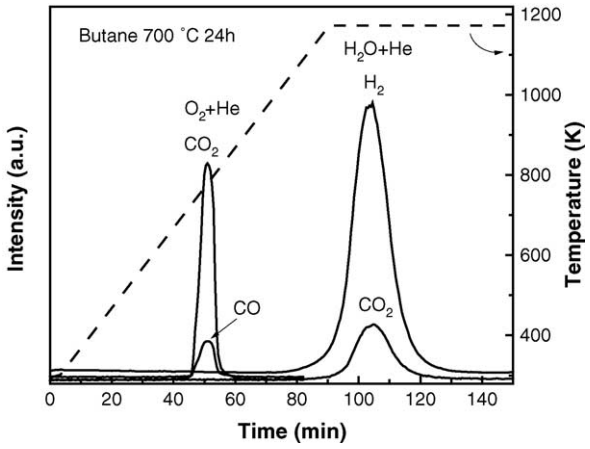

Fig. 7. Comparison of TPO curves in O_2 (20 vol.%) + He and steam (20 vol.%) + He with samples of porous YSZ/CeO_2 exposing to *n*-butane at 973 K for 24 h.

for 0.5 h, to 3.8 wt.% for 5 h, 10 wt.% for 24 h and then to 15 wt.% for 90 h exposures.

To determine the type of the deposits by GC–MS that formed on the porous anodes would be difficult in that the carbonaceous deposits were already stabilized after 1173 K and not soluble. It should be noted that the types of compounds analyzed in previous work [17] are only those soluble in toluene, where the deposits formed on a Cu plate after exposure to *n*-butane at 973 K for 24 h are aromatic, most with multiple, conjugated aromatic rings. There are some compounds that cannot be dissolved still keeping unknown. Therefore, TPO-O_2 measurements were conducted to study the stability of the carbonaceous compounds after different time exposure. The oxidizing gas consisted of 20% O_2 in a He carrier. Products and O_2 consumption were monitored using a mass spectrometer. Most of the products were CO_2 and less amount of CO were also produced. The curves of CO_2 products ($m/e = 44$) were shown in Fig. 6 with the exposure time to *n*-butane at 973 K marked on each peak. In accordance with the results in Fig. 5, the amount of deposits continuously increased over the time period according to the increased area of each curve. In the mean time, the stability of the deposits increased with exposure time as shown by the fact that the oxidation temperature increased, which also indicates the changes of the type of compounds.

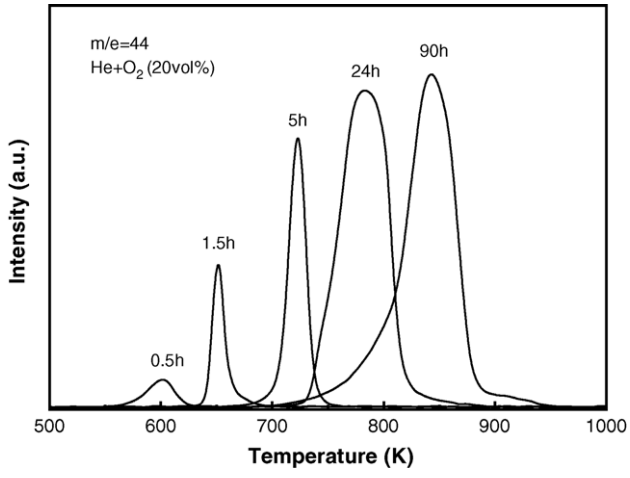

Fig. 6. TPO curves in 20 vol.% O_2 + He with samples of porous YSZ/CeO_2 exposing to *n*-butane at 973 K for different times.

Under practical operating conditions, most of the fuels will have been oxidized prior to the cell exit. The fuel will be diluted by steam and CO_2, it is important to know the conditions at which the carbonaceous compounds will be avoided or remain stable in steam. Therefore, TPO-H_2O measurements were conducted by using steam as oxidizing agent instead of O_2 with samples of porous YSZ slab containing 20 wt.% ceria after exposing to *n*-butane at 973 K for different times. Water was pumped to the reactor and kept at 20 vol.% steam in a He carrier. Products with increasing temperature were monitored using a mass spectrometer. It was found that the deposits can also be removed by steam and most of the products are H_2 and some CO_2, but the reaction temperature was greatly evaluated. Even for 0.5 h exposure to *n*-butane at 973 K, the reaction temperature was found to be over 1073 K. Fig. 7 shows a comparison of TPO curves in O_2 and steam with samples exposing to *n*-butane at 973 K for 24 h. While the deposits were removable by O_2 at ~780 K, the temperature was severely elevated in the case of steam, which was found to be over 1173 K. It was assumed that the carbonaceous deposits can also be removed at 973 K by steam but the amount of deposits will be controlled by the speed of removal and formation from the gas phase reaction.

4. Conclusions

The effects and nature of carbonaceous deposits formed in fuel cell anode compartment were investigated. While poor connectivity of Cu because of sintering can be compensated

by deposition of carbon upon short-term exposure of the anode to butane, too much deposit can deteriorate the fuel cell performance. The amount and stability of carbonaceous deposits increased with exposure time to *n*-butane. A dense layer of poly-aromatic rings formed from gas phase reaction at 973 K or above can block the fuels feeding and ions transfer and finally will shut down the fuel cell. The carbonaceous deposits can be removed by both O_2 and steam but the oxidation temperature was severely elevated for the case of steam, and the amount of deposits was controlled by the speed of removal by steam and formation from the gas phase reaction.

Acknowledgement

This work was funded by Defense Sciences Office of the Defense Advanced Research Projects Agency under the Palm Power Program.

References

[1] N.Q. Minh, J. Am. Ceram. Soc. 76 (1993) 563–588.
[2] R.M. Ormerod, Chem. Soc. Rev. 32 (2003) 17–28.
[3] C.V. Bartholomew, Catal. Rev.-Sci. Eng. 24 (1982) 67–112.
[4] T. Takeguchi, Y. Kani, T. Yano, R. Kikuchi, K. Eguchi, K. Tsujimoto, Y. Uchida, A. Ueno, K. Omoshiki, M. Aizawa, J. Power Sources 112 (2002) 588–595.
[5] K. Sasaki, Y. Teraoka, J. Electrochem. Soc. 150 (2003) A878–A884.
[6] S. Park, J.M. Vohs, R.J. Gorte, Nature 404 (2000) 265–267.
[7] R.J. Gorte, S. Park, J.M. Vohs, C. Wang, Adv. Mater. 12 (2000) 1465–1469.
[8] R.J. Gorte, J.M. Vohs, J. Catal. 216 (2003) 477–486.
[9] H.P. He, Y.Y. Huang, J.M. Vohs, R.J. Gorte, Solid State Ionics 175 (2004) 171–176.
[10] O.A. Marina, C. Bagger, S. Primdahl, M. Mogensen, Solid State Ionics 123 (1999) 199–208.
[11] A. Sauvet, J.T.S. Irvine, Fuel Cells 1 (2001) 205–210.
[12] H. He, Y. Huang, J. Regal, M. Boaro, J.M. Vohs, R.J. Gorte, J. Am. Ceram. Soc. 87 (3) (2004) 331–336.
[13] Y. Matsuzaki, I. Yasuda, Solid State Ionics 152 (2002) 463–468.
[14] H. He, J.M. Vohs, R.J. Gorte, J. Electrochem. Soc. 150 (2003) A1470–A1475.
[15] S. McIntosh, H. He, S.-I. Lee, O. C-Nunes, V.V. Krishnan, J.M. Vohs, R.J. Gorte, J. Electrochem. Soc. 151 (2004) A604–A608.
[16] S. McIntosh, J.M. Vohs, R.J. Gorte, Electrochim. Acta 47 (2002) 3815–3821.
[17] S.-I. Lee, S. McIntosh, J.M. Vohs, R.J. Gorte, in: S.C. Singhal, M. Dokiya (Eds.), Proceedings of the SOFC VIII, The Electrochemical Society Proceedings Series, PV 2003-07, Pennington, NJ, 2003, p. 865.
[18] S. McIntosh, J.M. Vohs, R.J. Gorte, J. Electrochem. Soc. 150 (2003) A470–A476.
[19] M. Boaro, J.M. Vohs, R.J. Gorte, J. Am. Ceram. Soc. 86 (2003) 395–400.